



Ferroelectric properties of $\text{Cd}_{1-x}\text{Zn}_x\text{Te}$ solid solutions

L. Benguigui, R. Weil, E. Muranevich, A. Chack, E. Fredj, and Alex Zunger

Citation: *Journal of Applied Physics* 74, 513 (1993); doi: 10.1063/1.355262

View online: <http://dx.doi.org/10.1063/1.355262>

View Table of Contents: <http://scitation.aip.org/content/aip/journal/jap/74/1?ver=pdfcov>

Published by the [AIP Publishing](#)

Articles you may be interested in

[Synthesis of \$\text{Zn}_x\text{Cd}_{1-x}\text{S}\$ Solid Solution by Stratified Method](#)

AIP Conf. Proc. 833, 116 (2006); 10.1063/1.2207088

[Electrophysical properties of semimagnetic solid solutions \$\text{Hg}_{1-x}\text{Mn}_x\text{Te}\$](#)

Low Temp. Phys. 30, 904 (2004); 10.1063/1.1820021

[Critical stress of \$\text{Hg}_{1-x}\text{Cd}_x\text{Te}\$ solid solutions](#)

J. Vac. Sci. Technol. B 10, 1451 (1992); 10.1116/1.586270

[Electroreflectance studies in \$\text{Cd}_{1-x}\text{Mn}_x\text{Te}\$ solid solutions](#)

J. Appl. Phys. 52, 4189 (1981); 10.1063/1.329233

[Crystal growth of \$\text{Zn}_x\text{Cd}_{1-x}\text{Te}\$ solid solutions and their optical properties at the photon energies of the lowest band gap region](#)

J. Appl. Phys. 44, 3659 (1973); 10.1063/1.1662816

Ferroelectric properties of Cd_{1-x}Zn_xTe solid solutions

L. Benguigui, R. Weil, E. Muravevich, A. Chack, and E. Frey
Solid State Institute and Physics Department, Technion-Israel Institute of Technology,
Haifa 32 000, Israel

Alex Zunger
National Renewable Energy Laboratory, Golden, Colorado 80401

(Received 13 January 1993; accepted for publication 18 March 1993)

Measurements of the spontaneous polarization P , x-ray diffraction, birefringence, dielectric constant at different frequencies, and specific heat C_p of the Cd_{0.9}Zn_{0.1}Te alloy are presented.

The results demonstrate that this system exhibits a diffuse, second-order ferroelectric transition.

(a) the ordering parameter is proportional to the square root of the temperature difference from the paraelectric phase; (b) the heat capacity is given by $C_p = (T_c/C) |(PdP/dT)|$, where C is the Curie constant. One of the main phenomena observed in these solid solutions is the instability of the ferroelectric phase. Once the neighborhood of the transition temperature is reached, the

terms of a two-state configuration coordinate diagram

I. INTRODUCTION

found to be ferroelectric. This is the first example of ferroelectricity (FE) in zinc-blende-based systems. The experimental evidence for such a conclusion was the behavior of the dielectric constant as a function of temperature and

ferroelectricity in these solid solutions was given by x-ray diffraction^{2,3} and by birefringence measurements.⁴ The x-ray-diffraction measurements provide an unambiguous proof of a phase transition through the determination of

blende structure and that the low-temperature phase is

ferroelectric properties of the Cd_{1-x}Zn_xTe solid solutions; (ii) show that different quantities, such as the polarization, the specific heat, and the birefringence, can be related to one another as observed in other ferroelectrics; (iii) give measurements of the dielectric constant at different frequencies; and (iv) discuss the instability of the ferroelectricity in terms of a configuration coordinate model. It can

does not exhibit FE at any temperature, and one that does (below a transition temperature). Indeed, while as-grown samples usually exhibit ferroelectricity, samples heated just

to reorganization of ferroelectric domains is the determination of the structure by x-ray diffraction: After heating, these samples have a cubic structure at room temperature.

We will suggest a hypothesis for this type of behavior in terms of a two-state model. Its clarification is a subject for

II. EXPERIMENTAL DETAILS

Single Cd_{0.9}Zn_{0.1}Te crystals were grown by the modi-

We do not use any procedure to polarize the samples. The samples were cut from the grown crystal, polished, and kept in darkness for some days before beginning the measurements. When needed, metal contacts were prepared by electroless deposition of gold from a gold chloride solution,

etched in a 5% Br in methanol solution for about 30 s. This procedure yielded low-resistance contacts with essentially linear $I-V$ curves. The equipment used to heat or cool the samples is standard and we shall only give a brief de-

III. POLARIZATION VERSUS TEMPERATURE

integration of the pyroelectric coefficient proposed by Chynoweth⁸ to which we have applied a new analysis. The first method can be used at low temperatures, but is of

a hot sample (direction $[111]$) is illuminated by a modulated light from a Ne-He laser beam. The direction of the polarization, as deduced from previous measurements,¹ was $\langle 111 \rangle$. The current produced in the samples can have

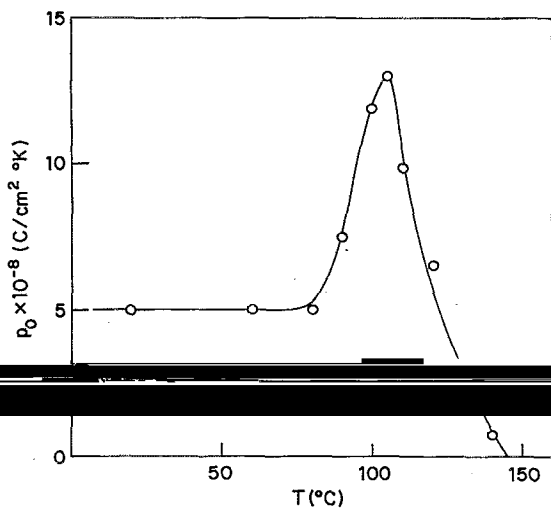


FIG. 1. Pyroelectric coefficient p_0 vs temperature T .

three origins: the photoelectric effect, the thermoelectric effect, and the pyroelectric effect. The photoelectric current is eliminated by covering the illuminated gold electrode with graphite. At the same time, we are assured that all the light is absorbed and heats the sample. Appendix A^{9,10} describes the method that allows the distinction and separation of the two other contributions: thermoelectric and

roelectric coefficient measured on a sample in which the pyroelectric current is much larger than the thermoelectric current. The pyroelectric coefficient p_0 is deduced from expression (A5) in Appendix A, using the value of the heat capacity obtained independently (see Sec. VII below). Note the peak in $p(T)$ at $T=105^\circ\text{C}$. Figure 2 shows the polarization P vs T , as determined from the two methods: directly from the hysteresis loop and from integration of the pyroelectric coefficient $p_0(T)$ (with the reasonable as-

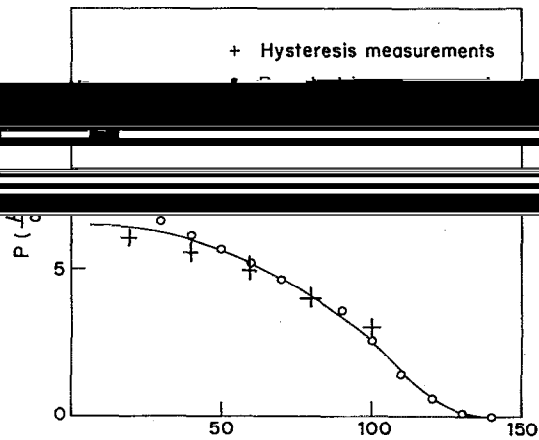


FIG. 2. Temperature dependence of polarization P as obtained from two different techniques: hysteresis loop and integration of the pyroelectric coefficient.

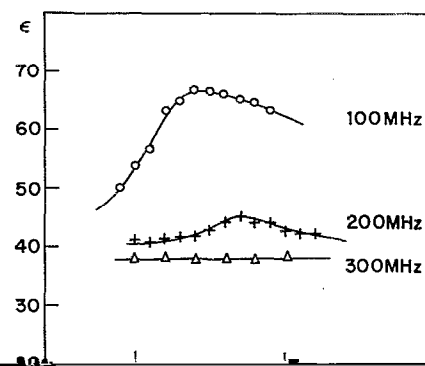


FIG. 3. Temperature dependence of dielectric constant ϵ at different frequencies. Note that at 300 MHz the transition is no longer visible.

sumption that $p=0$ at $T=140^\circ\text{C}$; see Fig. 1). There is a good agreement between the two curves when both methods are used at $T < 100^\circ\text{C}$. The curve deduced from p_0 shows clearly that the transition is diffuse, rather than sharp, in accordance with the measurements of the dielectric constant.¹

In Ref. 1, measurements of the dielectric constant ϵ have been presented at a single frequency of 100 MHz. In the present investigation, the measurements are extended up to 300 MHz. We used a Hewlett Packard model 8508A vector voltmeter associated with a reflectometer. The experimental setup is computerized. Figure 3 shows $\epsilon(T)$ at three frequencies (100, 200, and 300 MHz) for T around the transition temperature. The frequency has a strong effect on the amplitude of ϵ : It decreases as the frequency increases. At 300 MHz, the transition is no longer visible. At the same time, the maximum in $\epsilon(T)$ is shifted to a higher temperature when the frequency increases. These observations are similar to those noted in other ferroelectric solid solutions such as $\text{Pb}(\text{Zr}, \text{Ti})\text{O}_3$ and

The absolute value of the slope $d\epsilon/d\omega$ is maximum for a frequency equal to the inverse of a characteristic time τ . In an ideal ferroelectric this time is the relaxation time associated with the polarization dynamics,¹² but for a diffuse transition it has been shown¹³ that there is a distribution of relaxation times and τ is a mean value of the distribution. In our case, a strong decrease of ϵ appears between 100

$(2\omega \times 10^8)^{-1}$ and $(6\omega \times 10^8)^{-1}$, i.e., $\tau \sim 10^{-9}$ s. This relatively high relaxation time is indicative of an order-disorder transition.¹²

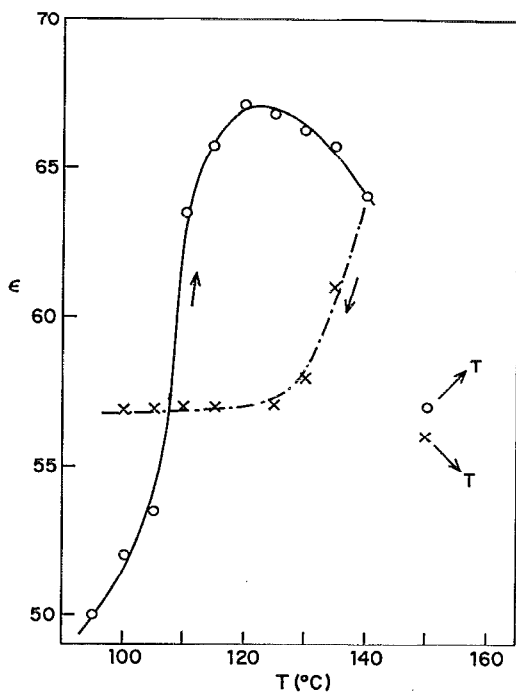


FIG. 4. Dielectric constant ϵ as a function of temperature T at 100 MHz on heating (O) and cooling (X) the sample. During cooling, one does not observe the anomaly in ϵ .

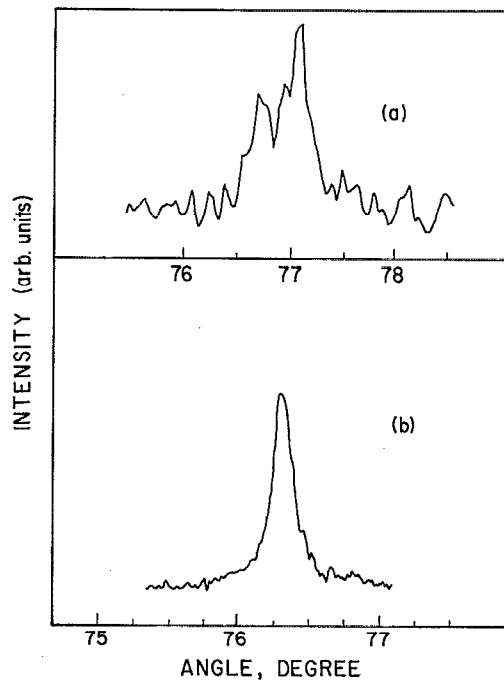


FIG. 5. Powder-x-ray-diffraction line [511] of $\text{Cd}_{0.9}\text{Zn}_{0.1}\text{Te}$ at 35°C (a) before heating and (b) after quenching from 100°C.

100 MHz. In the cooling cycle, we did not observe the maximum in ϵ which was observed during heating. This behavior is characteristic of a ferroelectric transition in our sample. The behavior of Fig. 4 is similar to that of

is evident. Figure 7 displays the temperature coefficient $(d\epsilon/dT)/\epsilon$ as a function of temperature. The maximum in $(d\epsilon/dT)/\epsilon$ is due to the anisotropy of the transition. The anisotropy is

even if there was a new domain distribution, we should have observed a peak in $\epsilon(T)$. This point is developed in Appendix B.¹⁴ We conclude that the absence of a transition once the sample had been heated to T_c does not result from domain reorientation.

As was the case for the dielectric constant, polarization measurements and the split x-ray-diffraction peak, the birefringence too disappeared during the second heating of the sample. We have been able to restore the ferroelectric state in some samples by an annealing procedure at about 700°C under a Te atmosphere (to preserve stoichiometry).

V. X-RAY DIFFRACTION

Powder-x-ray-diffraction measurements were conducted both below and above the ferroelectric transition temperature. The diffraction peaks of the zinc-blende structure are split below the transition temperature, and

not reproduced. The splitting is consistent with a rhombohedral distortion with an angle of 89.4 ± 0.1 . Marbeuf *et al.*³ have also found a rhombohedral distortion, with an angle of 89.94° . The splitting was resolved in the experimental spectra for all compositions in the range $x = 0.04$ to

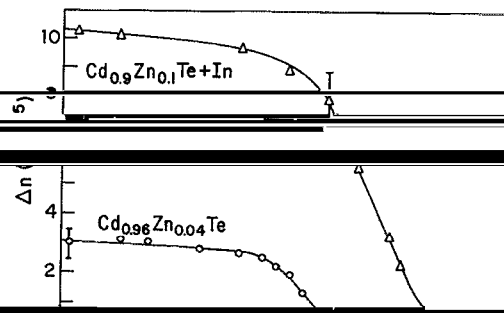


FIG. 6. Birefringence Δn vs temperature T for two samples: $x=0.04$ and

The birefringence of $\text{Cd}_{1-x}\text{Zn}_x\text{Te}$ was measured¹⁵ at a

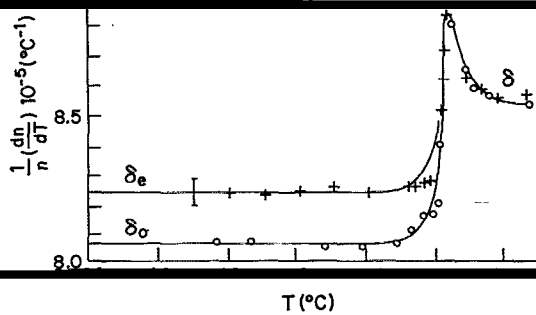


FIG. 7. Temperature dependence of $\delta = (dn/dT)/n$ for the ordinary (δ_o) and extraordinary (δ_e) refraction indices for the $\text{Cd}_{0.9}\text{Zn}_{0.1}\text{Te}$ sample.

We still do not control the procedure to our satisfaction, and research on a more reproducible and reversible procedure is continuing.

We next consider the dependence of Δn on polarization. Two cases are possible¹⁶ depending on whether the high-temperature phase is piezoelectric: (i) If the high-temperature (paraelectric) phase is nonpiezoelectric then $\Delta n \sim P^2$; here, (dn/dT) can exhibit either a jump (if the transition is sharp) or a smooth variation (if the transition is diffuse); (ii) If the high-temperature (paraelectric) phase is piezoelectric $\Delta n \sim P$; here (dn/dT) exhibits either a maximum (if the transition is sharp), or a minimum (if the transition is diffuse).

In our case, the high-temperature phase has the cubic zinc-blende structure (as checked by x-ray diffraction) which is piezoelectric. We find a maximum in (dn/dT) (Fig. 7), hence, the transition is of second-order type, but

we get a straight line for temperature above 80 °C. The reason for the deviation from the straight line at lower

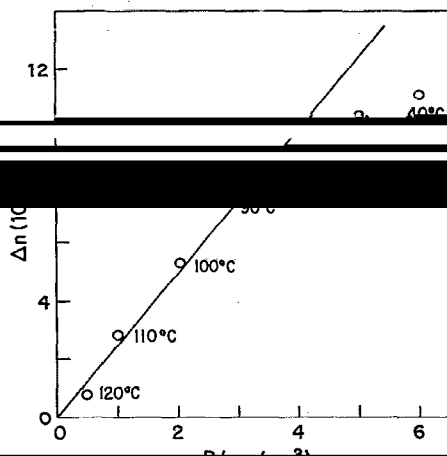


FIG. 8. Birefringence n vs polarization P curve showing the linearly

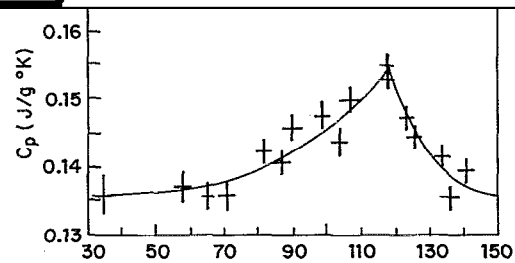


FIG. 9. Variation of the specific heat C_p with temperature T .

VII. SPECIFIC HEAT VERSUS TEMPERATURE

The specific heat was measured as follows: We took a small $\text{Cd}_{0.9}\text{Zn}_{0.1}\text{Te}$ sample ($1.1 \times 1.6 \times 1 \text{ mm}^3$) and covered its face with graphite. This face was exposed to a CO_2 laser beam. The intensity was varied with time as a step function: $I=0$ for $t < 0$; $I=\text{const}$ for $t > 0$. If the heating is uniform and there are no losses, the temperature increase should be linear with time with the slope $(dT/dt) = I/(mC_p)$, where C_p is the specific heat at constant pressure. When there are heat losses, the slope decreases with time, but it is still a good approximation to suppose that at $t=0$ the slope is given by the above expression. $C_p(T)$ was de-

termined by measuring the slope of the temperature increase at $t=0$. The problem, taking into account that the heating in the sample is not uniform, shows that the error is about 5%.¹⁴ Hence, the method we used has the advantage of simplicity but it is not very precise.

In Fig. 9, the variation of C_p with the temperature is shown. The behavior is consistent with a diffuse transition

which would have been either a step (mean-field transition)

VIII. RELATION BETWEEN SPECIFIC HEAT AND POLARIZATION

In ferroelectrics, the Landau-Devonshire (LD) theory¹⁶ gives a good phenomenological analysis of the experimental observations for sharp second-order transitions. In our case, the transition is diffuse as a result of the disorder previously shown. Outside the transition region our results are in accordance with a mean-field second-order phase transition (as given by the LD theory): $P^2 \propto (T_c - T)$ and the ratio of the slopes $(d\epsilon^{-1}/dT)$ above and below T_c is very nearly 2.

From the LD expansion¹⁶ of the free energy

$$G = G_0 + \frac{1}{2}\beta(T - T_c)P^2 + \gamma P^4, \quad (1)$$

it is possible to show that the heat capacity is related to the polarization by

$$C_p - C_p^0 = -T\beta P \frac{dP}{dT} \quad (2)$$

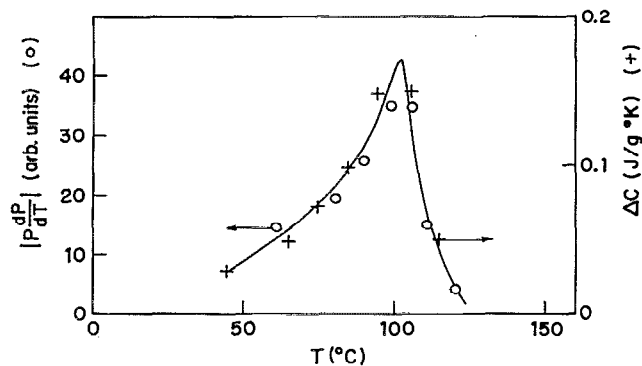


FIG. 10. Excess specific heat ΔC_p (crosses) and $|PdP/dT|$ (circles) vs temperature T mapped onto the same graph, showing the proportionality of the two quantities.

It has been noted¹⁷ that the relation (2) should also be valid for diffuse transitions. We shall thus apply Eq. (2) to our case.

Figure 10 shows that ΔC_p and $|PdP/dT|$ are proportional to each other. The Curie constant C is determined from the ΔC_p data and (b) an assumption that $C \propto T_c$ (see Fig. 9) and $C \propto T_c^2$ (see Fig. 10).

Figure 10 shows that ΔC_p and $|PdP/dT|$ are proportional to each other. The Curie constant C is determined from the ΔC_p data and (b) an assumption that $C \propto T_c$ (see Fig. 9) and $C \propto T_c^2$ (see Fig. 10).

We found $(P/T_c) \approx 2$ compared with $C/T_c = 2.11$ deduced from the dielectric measurements for the 10% sample. The agreement is very good (probably accidental). Thus formula (2), which links the Curie constant, the specific heat, and the polarization, is verified in this diffuse transition.

IX. DISCUSSION

The measurements presented in this article, i.e., polarization, specific heat, birefringence, dielectric constant, and the x-ray diffraction give a picture of the ferroelectricity in

ature is about $5 \mu\text{C}/\text{cm}^2$, this is comparable to the values

solutions behave as regular ferroelectrics. However, it is necessary to explain why a small amount of Zn gives such a high transition temperature. Only 4% of zinc gives $T_c \approx 90^\circ\text{C}$ (363 K). This can be compared with an analogous system $\text{Pb}_{1-x}\text{Ge}_x\text{Te}$ for which $x = 16\%$ corresponds only to $T_c \approx 220$ K.¹⁸

A central hallmark of the ferroelectricity in this system is its dependence on the thermal history. For example,

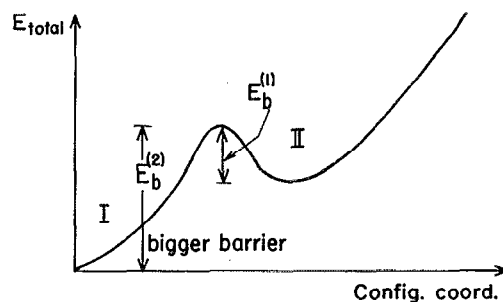


FIG. 11. Schematic configuration-coordinate diagram illustrating the proposed two-state system.

frequency dielectric peak (Fig. 5) and a specific-heat peak (Fig. 9) at T_c , and a splitting of the zinc-blende diffraction peak below T_c (Fig. 5), once the neighborhood of the transition temperature is reached, most of the time, subsequent cooling leads to the disappearance of these effects. Furthermore, heating again the samples that have reached

electric behavior can be restored in some samples by a

These effects are not understood at the present time. It is

distinct nonequilibrium states, one (state I) that does not

an ordinary zinc-blende solid solution that is nonferroelectric, while the system in state II could correspond to a statically deformed lattice whose lower overall symmetry (see the x-ray data) permits ferroelectricity. The two states can be thought of as two distinct minima in a configuration-coordinate diagram. These minima can be

schematically in Fig. 11. This qualitative model can then be used to speculate on the nature of the unstable ferroelectricity in CdZnTe, as follows: Samples whose thermal history or growth conditions placed them in state II (e.g.,

when heated sufficiently to overcome the barrier E_b , part

the ferroelectricity. These particles can be released only if the sample is annealed at a temperature $T \gg T_c$ to overcome the larger barrier $E_b^{(2)}$.

To search for a microscopic model that could result in such a situation, we have studied theoretically¹⁹ off-center atomic displacements in ordinary zinc-blende semiconductors. A "supercell," consisting of four cations and four anions, originally placed at the zinc-blende atomic positions, was considered. The total energy was calculated as a function of the displacement of the four cations and the four anions.

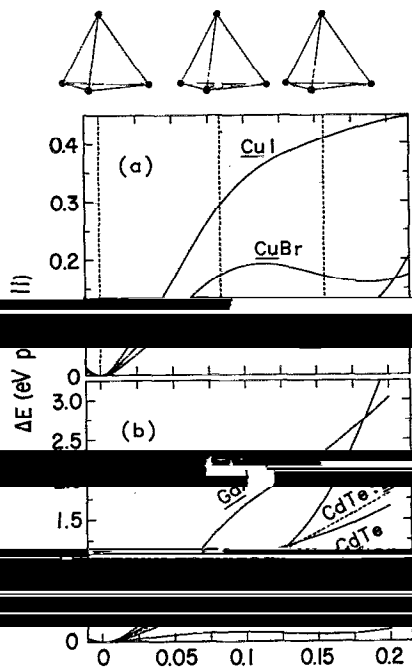


FIG. 12. Results of first-principles LAPW total energy calculations illustrating the off-center behavior in some zinc-blende semiconductors.

linearly augmented plane wave (LAPW) method.²¹ A single cation atom was then displaced from the tetrahedral site (direction), resulting in a C_{3v} symmetry (see the x-ray study

Fig. 12. We see that for a system with active cation d orbitals such as CuCl, there exists indeed a secondary, off-center minimum, as envisioned in Fig. 11. The details of the microscopic mechanism leading to this instability

bands and the empty s conduction bands (the "pseudo-Jahn-Teller" effect)—will be discussed in a future publication.¹⁹

As pointed out by Bersuker *et al.*,²² the t_2 -type normal-mode displacements in Td tetrahedral systems induce a dipole. In state II there are four local-equilibrium configurations corresponding to the four bond directions. In each minima, the dipole coincides with the direction of the bond. At high temperatures (as long as the system is in state II) the system jumps dynamically between these minima through tunneling. The observed net dipole will then depend on temperature and tunneling rate. In the absence of correlation between the tetrahedra, the system as a whole will be unpolarized. As the temperature is lowered, the dipole correlation is enhanced and a net polarization will appear as a result of an order-disorder transition. Note that the ferroelectricity in such a system is metastable ferroelectricity, since the true ground state has the nonferroelectric zinc-blende structure.

Since the off-center displacement found in CuCl derives from a metal d orbital, it is expected to be much

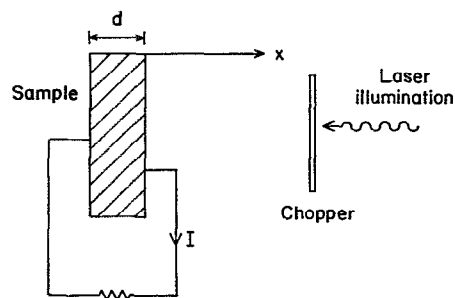


FIG. 13. Schema of the pyroelectric and thermoelectric measurements.

studies show that CuCl has d bands near the top of its valence band,²³ II-VI compounds have considerably deeper

strong anharmonicities, but no distinct secondary mini-

skin to the disordered alloy environment could lead to a metastable minimum. Hence, while the conceptual model envisioned in Fig. 11 seems applicable to I_B -VII systems, direct evidence for its applicability to II-VI systems is lack-

experimental research: characterize the preparation conditions, thermal treatment, or photoinduced effects that maximize the population of state II, hence the amplitude of the

in their vibrational properties (as was seen by Livescu and

bands, polarization, birefringence, etc. Furthermore, if the dipoles in this system are induced by the Cd-Zn size difference which leads to off-center displacements, a similar effect should be seen in other size-mismatched alloys, e.g.

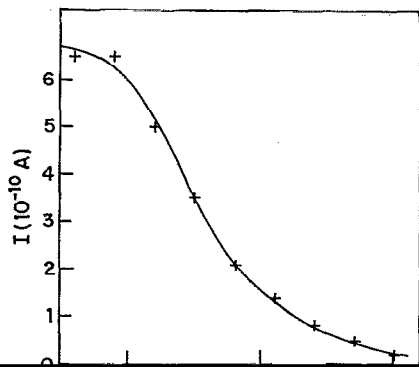
should be pursued.

ACKNOWLEDGMENTS

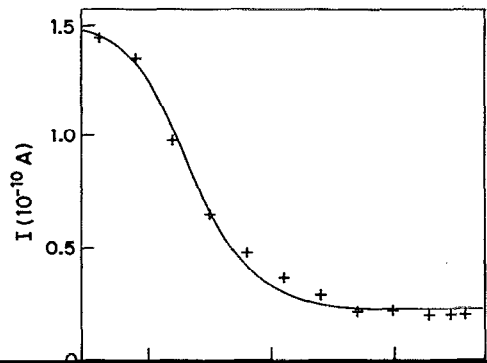
The technical help of A. Naaman and F. Kohn is acknowledged. This research was funded in part by Grant No. 89-00324 from the United States-Israel Binational Science Foundation (BSF), Jerusalem, Israel, and by the Center for Absorption in Science, Ministry of Immigrant Absorption, State of Israel.

APPENDIX A

The experimental situation for the measurement of the pyroelectric current is shown in Fig. 13. A slab (thickness d) is illuminated by a modulated laser beam [intensity $W_1 + W_0 \exp(j\omega t)$]. The thermal contact of the second face with the holder is characterized by a relaxation time τ . If other dimensions are larger than the thickness, the excess temperature will depend only on x and t . In the steady-state regime,⁹ T is equal to



Eq. (A3).



large frequencies the current goes toward a finite value. The line is a fit obtained using expressions (A3) and (A5).

$$\Delta T(x,t) = \frac{W_1}{C_p \rho d} \left[\frac{1}{1 + \gamma \omega \tau_1} + 2 \sum_{n=1}^{\infty} \cos\left(\frac{n\pi x}{d}\right) \exp\left(-\frac{n^2 \pi^2 \tau}{d^2} t\right) \right] \exp(i\omega t) \quad (A1)$$

In Eq. (A1), a constant term proportional to W_1 was not included since only the time-dependent part of ΔT was of interest. C is the heat capacity, ρ is the sample density, τ is

The thermoelectric current is equal to

$$I_{th} = (K/R) [\Delta T(x=0) - \Delta T(x=d)], \quad (A2)$$

where K is the thermoelectric power and R is the total resistance of the circuit. One obtains

$$I_{th} = \frac{4K W_1 \tau_1}{R} \sum_{n=1}^{\infty} \frac{1}{1 + \gamma \omega \tau_1} \exp\left(-\frac{n^2 \pi^2 \tau}{d^2} t\right) \cos\left(\frac{n\pi x}{d}\right) \exp(i\omega t) \quad (A3)$$

To verify the validity of this expression a sample of CdTe ($4 \times 5 \times 0.8 \text{ mm}^3$) was prepared, and I_{th} was measured as a

deduced from the fit and all the other known quantities is $250 \mu\text{V/K}$. It compares well with the results of Kubalkova for a n -type sample with $10^{14} \text{ holes/cm}^3$ as our CdTe sam-

$$I_{pyro} = \frac{S}{d} \int_0^d \frac{\partial \Delta T}{\partial t}(x,t) dx, \quad (A4)$$

surface) and p_0 is the pyroelectric coefficient. If I is small enough, p_0 can be taken constant through the sample. Using Eqs. (A1) and (A4) one has

$$I_{pyro} = \frac{S}{C_p \rho d} \frac{1}{1 + \gamma \omega \tau_1} \quad (A5)$$

total current is the sum of the two contributions.

The absolute value I_{th} is characterized by a monotonic decrease when ω increases from zero to ∞ . There is a simple and clear cut distinction between the two effects: A sample with a pyroelectric effect will give a finite value for the current at high frequencies.

In Fig. 15, a sample with the two contributions is shown. The results are fitted taking for the total current

frequency dependence. As shown in Fig. 15 by the solid line, the fit is very good.

In the course of this work, three kinds of $\text{Cd}_{0.9}\text{Zn}_{0.1}\text{Te}$

those with the thermoelectric current much larger than the pyroelectric one. The dependence of I on ω is similar to

APPENDIX B

of a ferroelectric crystal with a cubic paraelectric phase and a rhombohedral ferroelectric phase is

with $A = A_0(T - T_c)$ and $C > B$.

This last condition is necessary in order to insure that the rhombohedral ferroelectric phase will be the most sta-

deduced from the conditions

or

$$AP_x + BP_x^3 + CP_x(P_y^2 + P_z^2) = 0,$$

$$AP_y + BP_y^3 + CP_y(P_x^2 + P_z^2) = 0, \quad (B2)$$

$$AP_z + BP_z^3 + CP_z(P_x^2 + P_y^2) = 0.$$

The rhombohedral solution is $P_x = P_y = P_z = P_0$ with P_0 given by

$$A + (B + 2C)P_0^2 = 0. \quad (B3)$$

From Eq. (B3), one sees that P_0 varies as $(T_c - T)^{1/2}$.

Now we apply electric field (E_x, E_y, E_z) . From $dG/dP_x + E_x$ (and similar expressions for P_y and P_z), one finds (for $T < T_c$)

$$\begin{aligned} E_x &= 2BP_0^2\delta P_x + 2CP_0^2\delta P_y + 2CP_0^2\delta P_z, \\ E_y &= 2BP_0^2\delta P_y + 2CP_0^2\delta P_x + 2CP_0^2\delta P_z, \\ E_z &= 2BP_0^2\delta P_z + 2CP_0^2\delta P_x + 2CP_0^2\delta P_y, \end{aligned} \quad (B4)$$

with

$$P_x = P_0 + \delta P_x, \quad P_y = P_0 + \delta P_y, \quad P_z = P_0 + \delta P_z.$$

The components of the susceptibility tensor χ_{ij} are $\delta P_i/E_j$. From Eq. (B4) it is easy to see that all the $\chi_{i,j}$'s are proportional to P_0^{-2} ; therefore, they all diverge at T_c . Above T_c , χ is equal to $\chi_0 = (T - T_c)^{-1}$. Thus, we conclude that when measuring the dielectric constant by applying an electric field, an anomaly must always be observed at T_c . In our case, it means that an anomaly must always be

The slope $d\epsilon^{-1}/dT$ is dependent on the chosen direc-

the polarization.

¹R. Weil, R. Nkum, E. Muranevich, and L. Benguigui, Phys. Rev. Lett. **62**, 2744 (1989).
²R. Nkum, R. Weil, E. Muranevich, L. Benguigui, and G. Kimmel, Mater. Sci. Eng. B **9**, 217 (1991).
³A. Marbeuf, C. Mondoloni, R. Triboulet, and J. Rioux, Solid State Commun. **75**, 275 (1990).
⁴E. Fredj, R. Weil, E. Muranevich, and L. Benguigui, Ferroelectrics **125**, 483 (1992).
⁵J. T. Benhalal, R. Triboulet, R. Granger, D. Lemoine, and Y. Marguaton, J. Cryst. Growth **117**, 281 (1992).
⁶E. Muranevich, M. Roitberg, and E. Finkman, J. Cryst. Growth **64**, 285 (1983).
⁷A. Muso, J. P. Ponpon, J. J. Grob, M. Hage-Ali, R. Stuck, and P. Siffert, J. Appl. Phys. **54**, 3260 (1983).
⁸A. G. Chynoweth, Phys. Rev. **117**, 1235 (1960).
⁹S. Bauer and B. Ploss, in Proceedings of the 6th International Symposium on Electrets (ISE6), IEEE Conference Proceedings, Cat. No. 88CH2593-2, 1988, p. 28.
¹⁰S. Kubalkova, Phys. Status Solidi B **50**, 111 (1972).
¹¹L. E. Cross, Ferroelectrics **76**, 241 (1987).
¹²R. Blinc and B. Zeks, *Soft Modes in Ferroelectrics* (North-Holland/Elsevier, Amsterdam 1974).
¹³R. Mizeris and J. Grigas, Ferroelectrics **126**, 133 (1992).
¹⁴L. Benguigui, Solid State Commun. **11**, 825 (1972).
¹⁵E. Fredj, master's thesis, Technion, Haifa, 1991.
¹⁶F. Jona and G. Shirane, *Ferroelectric Crystals* (Pergamon, Oxford, 1962).
¹⁷L. Benguigui, Solid State Commun. **14**, 669 (1974).
¹⁸S. Takaoka and K. Murase, Phys. Rev. B **20**, 2823 (1979).
¹⁹S.-H. Wei, S. B. Zhang, and A. Zunger, Phys. Rev. Lett. **70**, 1639 (1993).
²⁰S.-H. Wei and H. Krakauer, Phys. Rev. Lett. **55**, 1200 (1985).
²¹A. A. Muranevskii, and M. L. Kabanovich, Sov. Phys. Solid State **11**, 1981 (1970).
²²and M. L. Cohen, Phys. Rev. B **20**, 1189 (1979).
²³S.-H. Wei and A. Zunger, Phys. Rev. B **37**, 8958 (1988); **43**, 1662 (1991).
²⁴J. L. Lippman and J. H. Wynn, Phys. Rev. Lett. **51**, 1012 (1983).